

RESEARCH

Open Access



Probiotic *Pediococcus pentosaceus* restored gossypol-induced intestinal barrier injury by increasing propionate content in Nile tilapia

Feifei Ding¹, Nannan Zhou¹, Yuan Luo¹, Tong Wang¹, Weijie Li¹, Fang Qiao¹, Zhenyu Du¹ and Meiling Zhang^{1*}

Abstract

Background Intestinal barrier is a dynamic interface between the body and the ingested food components, however, dietary components or xenobiotics could compromise intestinal integrity, causing health risks to the host. Gossypol, a toxic component in cottonseed meal (CSM), caused intestinal injury in fish or other monogastric animals. It has been demonstrated that probiotics administration benefits the intestinal barrier integrity, but the efficacy of probiotics in maintaining intestinal health when the host is exposed to gossypol remains unclear. Here, a strain (YC) affiliated to *Pediococcus pentosaceus* was isolated from the gut of Nile tilapia (*Oreochromis niloticus*) and its potential to repair gossypol-induced intestinal damage was evaluated.

Results A total of 270 Nile tilapia (2.20 ± 0.02 g) were allotted in 3 groups with 3 tanks each and fed with 3 diets including CON (control diet), GOS (control diet containing 300 mg/kg gossypol) and GP (control diet containing 300 mg/kg gossypol and 10^8 colony-forming unit (CFU)/g *P. pentosaceus* YC), respectively. After 10 weeks, addition of *P. pentosaceus* YC restored growth retardation and intestinal injury induced by gossypol in Nile tilapia. Transcriptome analysis and siRNA interference experiments demonstrated that NOD-like receptors (NLR) family caspase recruitment domain (CARD) domain containing 3 (Nlrc3) inhibition might promote intestinal stem cell (ISC) proliferation, as well as maintaining gut barrier integrity. 16S rRNA sequencing and gas chromatography-mass spectrometry (GC-MS) revealed that addition of *P. pentosaceus* YC altered the composition of gut microbiota and increased the content of propionate in fish gut. In vitro studies on propionate's function demonstrated that it suppressed *nlr3* expression and promoted wound healing in Caco-2 cell model.

Conclusions The present study reveals that *P. pentosaceus* YC has the capacity to ameliorate intestinal barrier injury by modulating gut microbiota composition and elevating propionate level. This finding offers a promising strategy for the feed industry to incorporate cottonseed meal into fish feed formulations.

Keywords Gut barrier injury, Gossypol, ISCs proliferation, Nlrc3, Propionate

*Correspondence:

Meiling Zhang

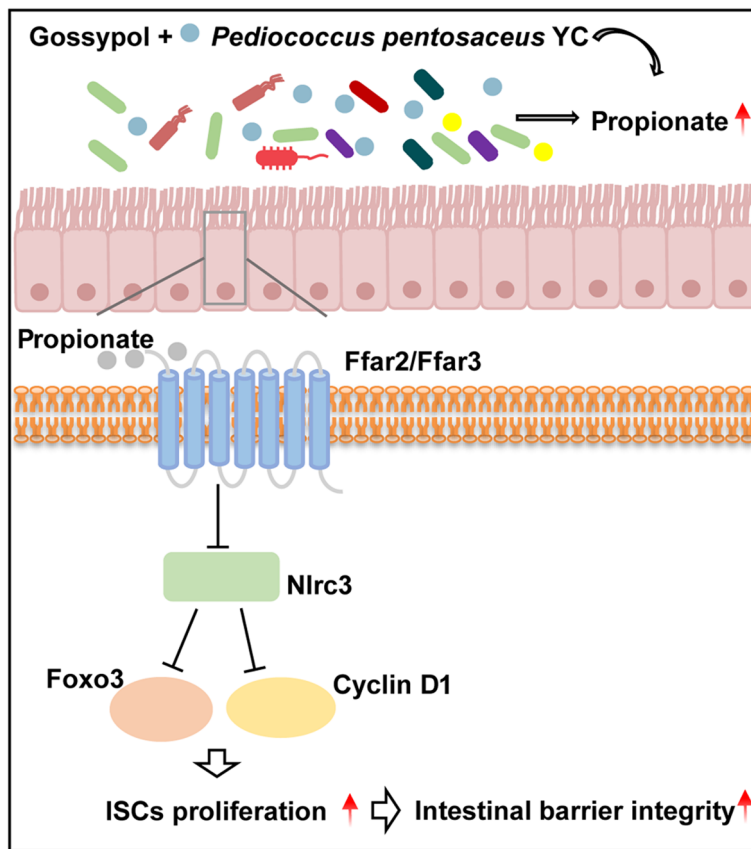
mlzhang@bio.ecnu.edu.cn

Full list of author information is available at the end of the article



© The Author(s) 2024. **Open Access** This article is licensed under a Creative Commons Attribution 4.0 International License, which permits use, sharing, adaptation, distribution and reproduction in any medium or format, as long as you give appropriate credit to the original author(s) and the source, provide a link to the Creative Commons licence, and indicate if changes were made. The images or other third party material in this article are included in the article's Creative Commons licence, unless indicated otherwise in a credit line to the material. If material is not included in the article's Creative Commons licence and your intended use is not permitted by statutory regulation or exceeds the permitted use, you will need to obtain permission directly from the copyright holder. To view a copy of this licence, visit <http://creativecommons.org/licenses/by/4.0/>. The Creative Commons Public Domain Dedication waiver (<http://creativecommons.org/publicdomain/zero/1.0/>) applies to the data made available in this article, unless otherwise stated in a credit line to the data.

Graphical Abstract



Background

The gastrointestinal tract acts as an important barrier to separate the body from the food components, antigens, intestinal microbiota and other possible toxins. It enables the absorption of nutrients and inhibits the invasion of the potentially harmful compounds or pathogens from the intestinal lumen [1–3]. It has been revealed that some dietary components or xenobiotics impair the intestinal barrier and disrupt the intestinal microbiota composition which in turn exacerbates this process [4, 5]. It has been established that the damage to the intestinal barrier is frequently accompanied by the activation of pro-inflammatory immune cells, then exacerbating the intestinal inflammation [6, 7]. And the impaired gut barrier is unable to prevent lipopolysaccharide (LPS) and other bacterial toxins from entering the circulatory system, thereby promoting hepatitis, hepatoma and meningitis [8–10]. Thus, the dysfunction or impairment of intestinal barrier will trigger intestinal disease or other multi-organ dysfunction syndromes [11].

The animal industry has confronted the challenge of escalating feed costs and the scarcity of protein resources [12, 13]. The cost of feed is largely attributed to the protein sources, so finding cheaper protein alternatives would be advantageous for both the industry and farmers. Cottonseed is one of the major products of cotton, with a global annual production of up to 26 million tons. Cottonseed meal (CSM) is a protein-rich product that can be found in large quantities and is typically more cost-effective compared to other protein sources such as fish meal (FM) and soybean meal (SBM) [14–16]. However, deepening researches have revealed that CSM especially the gossypol residue contained in CSM could cause severe intestinal inflammation and gut barrier injury in diverse monogastric animals such as fishes and livestock [13, 17–24]. Try to decrease the remaining gossypol in CSM is one of the important strategy to eliminate the deleterious effects [25, 26], but it depends on the dephenolization process which may

cause extra cost. Our previous research indicated that intestinal microbiota mediated the gossypol-induced gut barrier injury in Nile tilapia (*Oreochromis niloticus*) [21], thus we hypothesized that regulating intestinal microbiota may have the potential to repair gossypol-induced gut barrier injury.

Probiotics are initially employed as an economical and green substitute for antibiotics in feed additives [27, 28], and the Chinese Ministry of Agriculture and Rural Affairs has granted approval for the supplementation of animal feed with *Pediococcus pentosaceus*. Previous research elucidated that administration of *P. pentosaceus* CECT 8330 could increase the abundance of *Bifidobacterium* and *Lactobacillus* to strengthen mucosal integrity in DSS-induced colitis mice [29]. Addition of *P. pentosaceus* ZJUAF-4 restored gut microbiota composition against diquat-induced intestinal injury in mice [30]. *P. pentosaceus* PR-1 increased the abundance of *Fusobacteria*, *Cetobacterium* and *Plesiomonas* and reinforced gut barrier integrity in high-fat-diet-fed zebrafish (*Danio rerio*) [31]. The intestinal epithelium regenerates every 3–5 d to replenish the aged and damaged cells in the villi and ensure intestinal barrier integrity. Intestinal stem cells (ISCs) express the cell-surface markers, leucine-rich repeat-containing G-protein coupled receptor 5 (Lgr5) and olfactomedin 4 (Olfm4), and differentiate perpetually into intestinal epithelial cells, which governed the renewal of intestinal epithelium [32–35]. Addition of probiotics have been demonstrated to reinforce gut barrier integrity by promoting ISCs proliferation in mice [34, 36], but the exact mechanism by which *P. pentosaceus* repairs the injured intestinal barrier remains unclear.

Nile tilapia is the third most farming teleost fish worldwide [37] and CSM is regarded as the potential protein source for fish in near future. A bacterial strain (YC) affiliated to *P. pentosaceus* was isolated from the gut of Nile tilapia. *P. pentosaceus* YC was used to treat Nile tilapia exposed to gossypol and the restoration effect of *P. pentosaceus* on intestinal permeability was evaluated.

Methods

Bacteria strain and culture

The preserved strain *P. pentosaceus* YC, isolated from the gut of Nile tilapia [38], was recovered and spread on the Man Rogosa Sharpe (MRS)-agar plate (Basebio, Hangzhou, China). The bacterial suspension was identified by sequencing the full length of 16S rRNA gene

(Personalbio, Shanghai, China). The single colony of *P. pentosaceus* YC was cultured overnight in MRS medium at 28°C at 100 r/min for 18 h. Following centrifugation at 2,000 × *g* for 15 min, the bacterial precipitation was resuspended in sterile 1 × phosphate buffered saline (PBS) and mixed with the diet powder to form the pellets. The bacterial quantity was detected by serial dilution and counting on MRS agar plates.

Animal experiments

Juvenile Nile tilapia were purchased from Guangzhou Tianfa Fry Development Co., Ltd. (Guangzhou, China). All fish were raised in the environment with water temperature of 28°C, a dissolved oxygen higher than 6.0 mg/L, and light/dark cycle of 12 h/12 h. Fish were acclimated and fed with a commercial diet purchased from Tongwei Co., Ltd. (Chengdu, China) for 2 weeks. Two hundred and seventy Nile tilapia (2.20 ± 0.02 g) were randomly divided into nine 200-L tanks (30 fish/tank, 3 tanks/diet), fed with three diets including the CON (control diet), GOS (control diet containing 300 mg/kg gossypol) and GP (control diet containing 300 mg/kg gossypol and 10⁸ colony-forming unit (CFU)/g *P. pentosaceus* YC). During the experiment, fish were fed with gossypol for 8 weeks in GOS group, and fish were fed with *P. pentosaceus* YC daily for 2 weeks prior to the gossypol addition in GP group. All fish were fed twice (08:30 and 18:30) daily and fed at 4% of their average body weight within a day. The formulation of the diets was listed in Additional file 1: Table S1.

Sample collection

After the feeding trial, Nile tilapia were fasted for 16 h before sampling. Twelve fish were randomly selected from each group (4/tank) and anesthetized with 20 mg/L tricaine methanesulfonate (MS-222, E10521, Sigma-Aldrich, St. Louis MO, USA). The whole intestinal contents were collected for 16S rRNA sequencing, short chain fatty acids (SCFAs) and lactate quantification. Blood samples were drawn from the caudal part of fish and centrifuged at 3,000 r/min for 10 min at 4°C to obtain serum for LPS concentrations detection. Proximal intestine (PI) and distal intestine (DI) were separately stored at –80°C for gene expression quantification and transcriptome sequencing. The final body weight, liver, intraperitoneal fat and final body length of each fish were measured and the growth indicators and organ indices were calculated following the under formula:

$$\text{Weight gain (WG, g)} = \text{final body weight (FBW, g)} - \text{initial body weight (IBW, g)}$$

$$\text{Specific growth rate (SGR, \% / d)} = 100 \times [(\ln \text{ FBW} - \ln \text{ IBW}) / \text{time (d)}]$$

$$\text{Condition factor (CF, g/cm}^3\text{)} = 100 \times [\text{body weight (g)} / \text{body length}^3 \text{ (cm)}]$$

$$\text{Hepatosomatic index (HSI, \%)} = 100 \times [\text{liver weight (g)} / \text{body weight (g)}]$$

$$\text{Mesenteric fat index (MFI, \%)} = 100 \times [\text{mesenteric fat weight (g)} / \text{body weight (g)}]$$

Intestinal permeability assay

Intestinal permeability was detected by an Ussing chamber as previously described [39]. Six proximal intestine segments larger than 0.01 cm² from each group were directly rinsed with the buffer (NaCl, 140 mmol/L; NaHCO₃, 10 mmol/L; KCl, 4 mmol/L; NaH₂PO₄, 2 mmol/L; MgSO₄, 1 mmol/L; CaCl₂, 1 mmol/L; glucose, 5.5 mmol/L; pH 7.8) and fixed on a clamp. After an equilibration for 20 min, transepithelial electrical resistance (TEER) was automatically monitored in a 10-min-circuit current.

Histological analysis

The 4% paraformaldehyde-fixed proximal intestine samples were embedded in paraffin, and then cut into 5 μm slice for the hematoxylin and eosin (H&E) staining. A light microscope (Nikon Ds-Ri2, Nikon Corporation, Tokyo, Japan) was used to image the intestinal villus height, villus thickness and basal layer thickness from at least 24 segments. Quantification and statistical analysis were conducted according to the previous article by using imaging software (Nis-Elements F package version 4.60) [40].

Biochemical analysis

The LPS concentration in the serum was quantified by using fish LPS enzyme-linked immunosorbent assays (ELISA) kits (HB794-QT, Shanghai Hengyuan Biotechnology Co., Ltd., China). The levels of lactate in intestinal contents were measured using the commercial kit (A019-2-1, Nanjing Jiancheng Bioengineering Institute, Nanjing, China) according to the manufacturer's instruction.

Short chain fatty acids quantification

Total SCFAs in intestinal contents were determined using gas chromatography-mass spectrometry (GC-MS). Briefly, 0.02 g intestinal contents mixed with 200 μL 1 × PBS, acidified with 50 μL of 50% sulfuric acid and crushed by homogenizer (DLAB Scientific Co., Ltd., Beijing, China). 250 μL of diethyl ether was used

for SCFAs extraction. All operations were performed on ice. The Gas Chromatography Nexis GC-2010 (Shimadzu, Kyoto, Japan) was utilized to measure SCFAs levels according to the following program: temperature increased from 60 °C to 100 °C at a rate of 5 °C/min, for 2 min; increased to 180 °C at 5 °C/min for 2 min. The external standard method was employed in order to calculate the concentration of SCFAs (acetate, propionate and butyrate) (71251, 94425 and 19215, Sigma-Aldrich, St. Louis MO, USA).

Quantitative PCR (qPCR) analysis

Total RNA from tissues or cells was extracted using Tripure Reagent (RN0102, Aidlab, Beijing, China). The quality and quantity of RNA were determined by agarose gel electrophoresis and NanoDrop 2000 spectrophotometry (Thermo Scientific, Waltham, USA). Then the complementary DNA (cDNA) was synthesized using a FastQuant reverse-transcribed kit with gDNase (R323-01, Nanjing Vazyme Biotech Co., Ltd., Nanjing, China). Quantitative real-time PCR was performed on CFX96 Real-Time PCR system (Bio-Rad, Richmond, USA) using 2 × SYBR Master Mix (Q711-02, Nanjing Vazyme Biotech Co., Ltd., Nanjing, China) containing 10 μmol/L gene specific primer. Gene expression levels were calculated using 2^{-ΔΔCT} method and normalized to the housekeeping genes elongation factor 1 alpha (*ef1α*) and *β-actin*. The PCR primers were designed using NCBI Primer BLAST based on the NCBI database and synthesized by Shanghai Personal Biotechnology Co., Ltd. Primer sequences were summarized in Table S2.

RNAseq analysis

Total RNA from the distal intestine was extracted, qualified, paired and the purified RNA was used to construct the library using Illumina TruseqTM RNA sample prep kits. Paired-end sequencing was performed on the Illumina Novaseq 6000 sequencing platform (Majorbio, Shanghai, China). The gene expression levels were

quantitatively analyzed by RSEM software with TPM as the quantitative index. The differentially expressed genes (DEGs) were analyzed by DESeq2. Genes of P -value < 0.05 were considered as DEGs. Genes with detection values higher than 0.1 were used for Kyoto Encyclopedia of Genes and Genomes (KEGG) enrichment analysis and volcano plot analysis. The raw data was available in the NCBI with the BioProject accession number PRJNA987992.

Gut microbiota analysis

Genomic DNA extracted from the intestinal contents was performed by the Illumina NovaSeq 6000 System (Personalbio, Shanghai, China). Microbial composition was analyzed by targeting the V3–V4 region of 16S rRNA gene using primers 338 F (5'-ACTCCTACGGGAGGCAGCA-3') and 806 R (5'-GGACTACHVGGGTWCTCTAAT-3'). QIIME2 software was used to analyze sequencing reads. Alpha diversity indexes (Chao1, Shannon and Faith_pd) were significantly different among groups as assessed using the Kruskal-Wallis test. Beta diversity was conducted by the principal coordinate analysis (PCoA) based on Bray-Curtis distance. Linear discriminant analysis effect size (LEfSe) analysis was used to characterize taxonomic units with significant differences based on Wilcoxon test. Circos analysis was performed by the Genes cloud tools of Personalbio. The raw data of intestinal microbiota were available in the NCBI with the BioProject accession number PRJNA987999.

In vivo NOD-like receptors (NLR) family caspase recruitment domain (CARD) domain containing 3 (*nlrc3*) siRNA in the intestine of Nile tilapia

Three siRNA fragments of *nlrc3* (Gene ID: 100694916) were designed to target different encoding regions and the scrambled siRNA (Table S3) was administered to juvenile Nile tilapia (1.11 ± 0.02 g) as previously reported [41]. Briefly, 10 µL of 1 × PBS, siRNA scramble (50 µmol/L) and *sinlrc3* (50 µmol/L) were delivered into the etherized juvenile fish via oral gavage using 10 µL micro pipette tips. The siRNAs were given orally to the same fish every 2 d. Five fish in each group were dissected for mRNA expression analysis at 1 d and 7 d post-siRNA treatment.

Western blot

Intestinal tissues were homogenized on ice by using ice-cold radioimmunoprecipitation assay (RIPA) lysis buffer (P0013B, Beyotime Biotechnology, Shanghai, China) containing 1 mmol/L phenylmethylsulfonyl fluoride (PMSF) (ST506, Beyotime Biotechnology, Shanghai, China) for 30 min. The extracted protein

was mixed with 5 × sodium dodecyl sulfate (SDS) loading buffer and boiled at 95 °C for 10 min. The 100 µg protein was subjected to 10% sodium dodecyl sulfate polyacrylamide gel electrophoresis (SDS-PAGE). The protein concentration was determined using Bicinchoninic acid (BCA) assay Protein Assay kit (P0012, Beyotime Biotechnology, Shanghai, China). The antibodies were as follows: anti-Nlrc3 (DF13411, Affinity Biosciences, Jiangsu, China), anti- α -Tubulin (AF4651, Affinity Biosciences, Jiangsu, China), and the secondary antibody IRDye® 600CW and IRDye® 800CW (Li-Cor Biotechnology, Nebraska, USA). Visualization was carried out using Odyssey Clx (Li-Cor Biotechnology, Nebraska, USA) and the densitometric quantification was performed using Image Studio Lite Ver 5.2 software.

Caco-2 cell line culture and treatments

Briefly, Caco-2 cells were obtained from ATCC, maintained in medium (RPMI 1640, 20% FBS, 100 U/mL penicillin, 0.1 mg/mL streptomycin) in a humidified incubator (37 °C and 5% CO₂) and passaged every 2–3 d at 80% confluency. For gene expression detection, cells were incubated in 12-well plates with gossypol (20 µmol/L) and sodium propionate (SP) (1 mmol/L and 5 mmol/L) for 24 h. For wound-healing assay, cells were seeded in 12-well plates until reaching 90%–100% confluency. After serum starving, 10 µL pipette tip was used to make a scratch in cell monolayer. Cells were treated with gossypol (20 µmol/L) and SP (1 mmol/L and 5 mmol/L) for 72 h. An inverted light microscope (Nikon Ds-Ri2, Nikon Corporation, Tokyo, Japan) was used to image and the imaging software (Nis-Elements F package version 4.60) was used to measure the wound closure. The wound closure was calculated according to the formula: [(original area of wound – final area of wound)/original area of wound]/2.

Statistical analysis

Data were presented as mean ± standard error of mean (SEM). Shapiro–Wilk test and Levene's test were used to test the normality and the homogeneity of variances for all data. One-way analysis of variance (ANOVA) with Tukey's adjustment was used to compare the differences among groups and unpaired Student's t -test was conducted for the difference analyses between two groups in GraphPad Prism 8. A value of $P < 0.05$ was deemed statistically significant.

Results

The effects of *P. pentosaceus* YC on the growth performance

After the feeding trial, the growth parameters were recorded to analyze the effects of *P. pentosaceus* YC on the growth performance of Nile tilapia. The WG, SGR

and FBL were significantly decreased in GOS group when compared to the CON group, and they were significantly increased in GP group compared with the GOS group ($P < 0.05$, Table 1). The CF, HSI and MFI had no significant difference among three groups ($P > 0.05$, Table 1). Collectively, addition of *P. pentosaceus* YC enhanced the growth performance of Nile tilapia.

Addition of *P. pentosaceus* YC repaired gossypol-induced intestinal barrier injury

We further detected the intestinal barrier integrity of Nile tilapia. The TEER was significantly reduced in GOS group

and remarkably increased in GP group ($P < 0.05$, Fig. 1A). Consistently, serum LPS concentration was significantly increased in GOS group and decreased after the addition of *P. pentosaceus* YC ($P < 0.05$, Fig. 1B), suggesting an increase of intestinal barrier permeability [42, 43]. Dietary gossypol caused shedding of intestinal epithelial cells at the top of villi, while addition of *P. pentosaceus* YC ameliorated the epithelium damage (Fig. 1C). Gossypol significantly decreased villi height, villi width and basal layer thickness ($P < 0.05$), while addition of *P. pentosaceus* YC resulted in a remarkable improvement of these indicators ($P < 0.05$, Fig. 1D–F). These results indicated that addition of *P. pentosaceus* YC repaired gossypol-induced gut barrier injury in Nile tilapia.

Table 1 Effects of three diets on growth performance in Nile tilapia

Items	CON	GOS	GP
Initial body weight, g	2.20 ± 0.02	2.20 ± 0.02	2.20 ± 0.02
Weight gain, g	27.98 ± 0.43 ^a	24.78 ± 0.37 ^b	27.42 ± 0.05 ^a
Specific growth rate, %/d	3.19 ± 0.01 ^a	2.99 ± 0.03 ^b	3.14 ± 0.03 ^a
Final body length, cm	11.85 ± 0.21 ^a	10.52 ± 0.22 ^b	11.79 ± 0.13 ^a
Condition factor, g/cm ³	1.60 ± 0.04	1.53 ± 0.03	1.54 ± 0.02
Hepatosomatic index, %	2.32 ± 0.09	1.99 ± 0.12	2.01 ± 0.12
Mesenteric fat index, %	0.38 ± 0.05	0.29 ± 0.04	0.31 ± 0.04

Data are represented as mean ± SEM and analyzed by ANOVA with Tukey test.

^{a,b}Different lowercase letters indicated significant differences ($P < 0.05$)

Addition of *P. pentosaceus* YC increased the gene expression of tight junction proteins (tjps)

Epithelial cell tjps such as zona occludens 1 (*zo-1*), *occludin*, *cadherin1* and *claudin* supported the integrity of the gut barrier, and the decrease of their expression can lead to a higher permeability of the intestine [44, 45]. In this study, we found that the expression level of *zo-1* was significantly reduced in PI and DI when fish fed with gossypol ($P < 0.05$, Fig. 2A and E), but it was markedly elevated after addition of *P. pentosaceus* YC ($P < 0.05$, Fig. 2A and E). Moreover, the gene expression of *occludin* was significantly decreased in DI when fish fed with gossypol

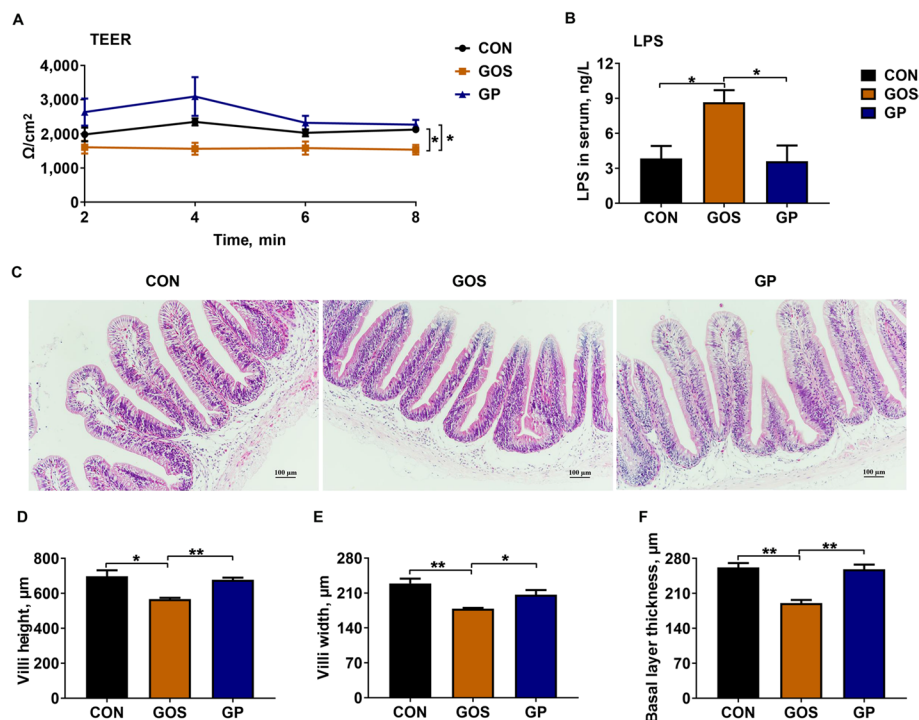


Fig. 1 Addition of *P. pentosaceus* YC repaired gossypol-induced intestinal barrier injury. **A** The TEER of intestine; **B** The LPS concentrations in serum ($n = 6$ individuals); **C** H&E staining of intestine; **D** Villi height; **E** Villi width; **F** Basal layer thickness ($n = 24$ individuals). Data are represented as mean ± SEM. Asterisk refers to the significant difference (ANOVA with Tukey's test; * $P < 0.05$, ** $P < 0.01$). CON, control diet; GOS, gossypol diet; GP, gossypol diet supplemented with *P. pentosaceus* YC; TEER, transepithelial electrical resistance; LPS, lipopolysaccharide

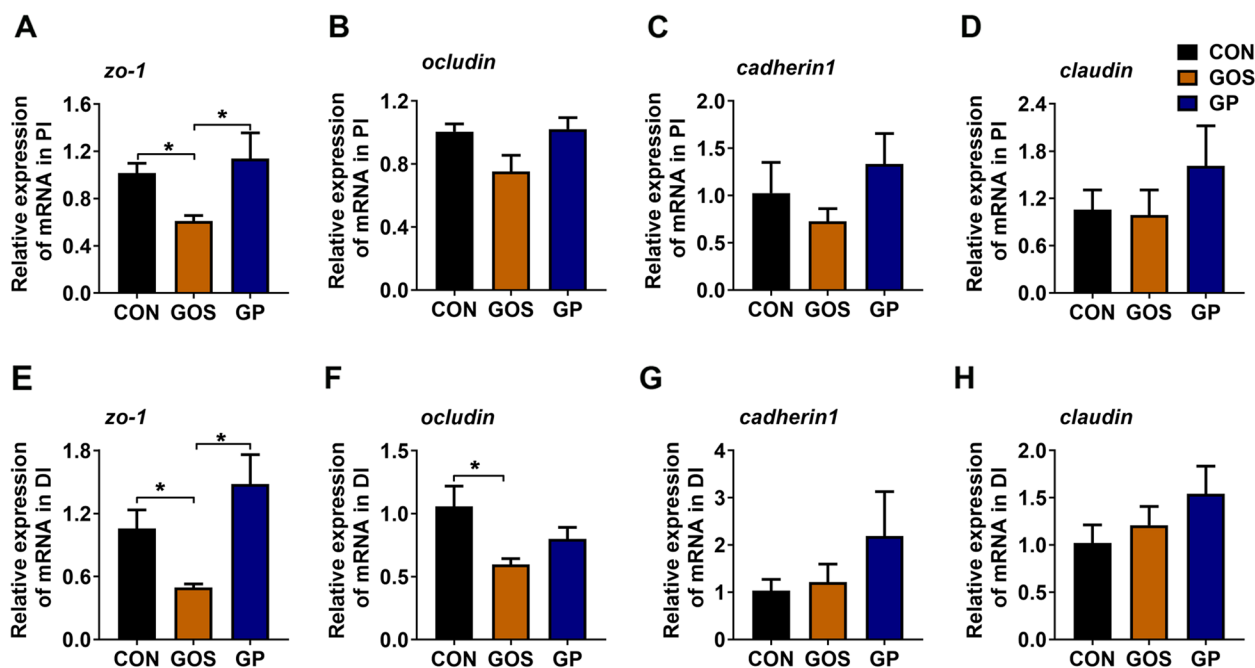


Fig. 2 Addition of *P. pentosaceus* YC promoted tjps expression. **A–D** The relative gene expression of *zo-1*, *occludin*, *cadherin1* and *claudin* in PI; **E–H** The relative gene expression of *zo-1*, *occludin*, *cadherin1* and *claudin* in DI ($n=6$). Asterisk refers to the significant difference (ANOVA with Tukey's test; * $P < 0.05$). CON, control diet; GOS, gossypol diet; GP, gossypol diet supplemented with *P. pentosaceus* YC; *zo-1*, zona occludens 1; PI, proximal intestine; DI, distal intestine

($P < 0.05$, Fig. 2F). There was no significant difference in the expression of *occludin* in PI ($P > 0.05$, Fig. 2B), *cadherin1* ($P > 0.05$, Fig. 2C and G) and *claudin* ($P > 0.05$, Fig. 2D and H) in PI and DI among three groups.

Addition of *P. pentosaceus* YC inhibited Nlr3 and promoted the gene expression of ISC markers

The RNAseq analysis was further used to explore the possible mechanism by which *P. pentosaceus* YC repaired gossypol-damaged intestinal barrier. The KEGG enrichment analysis enriched a shared NOD-like signaling pathway (Fig. 3A) which included 4 cell proliferation related genes (*nlr3*, forkhead box O3 (*foxo3*), *cyclinD1*, *cyclin G2*) and inflammatory related genes (inhibitor of nuclear factor kappa B kinase (*ikkb*), interleukin-1 β (*il-1\beta*)) (Fig. 3B). The expression of *nlr3* was significantly increased in GOS group and dramatically decreased in GP group ($P < 0.05$, Fig. 3B–D). The expression of *foxo3* and *cyclinD1* was significantly decreased in GOS group and remarkably increased in GP group ($P < 0.05$, Fig. 3B–D). We observed that dietary gossypol significantly decreased the expression of ISC marker genes *lgr5* and *olfm4* ($P < 0.05$, Fig. 3C), but addition of *P. pentosaceus* YC remarkably increased their expressions ($P < 0.05$, Fig. 3D), indicating *P. pentosaceus* YC administration might promote ISCs proliferation. The expression of ISC marker genes (*lgr5* and *olfm4*) (Fig. 3E and F), the

NOD-like signaling pathway related genes (*nlr3*, *foxo3* and *cyclinD1*) (Fig. 3 G–K) in PI and DI were confirmed by qPCR and Western blot, and the results were consistent with the transcriptome analysis. Together, these data indicated that addition of *P. pentosaceus* YC inhibited Nlr3 expression and promoted the gene expression of ISC markers.

Nlr3 was the key factor to regulate genes related to ISC markers

We designed a short-term experiment (*sinlrc3-3#* interference for 1 d) and a long-term experiment (*sinlrc3-3#* interference for 7 d) in vivo to detect how the inhibition of *nlr3* modulate the gene expression of ISC markers. *sinlrc3-3#* had the best inhibition effect of intestinal *nlr3* ($P < 0.05$, Fig. 4A), which was further used in both short-term and long-term experiments. The gene expression of *nlr3* was also significantly inhibited by *sinlrc3-3#* in the long-term experiment ($P < 0.05$, Fig. 4B). The expression levels of *foxo3*, *cyclinD1* were upregulated when *nlr3* was knock down ($P < 0.05$, Fig. 4C and F), suggesting that the expression of *foxo3* and *cyclinD1* could be influenced by *nlr3*. The gene expression of ISC markers (*lgr5* and *olfm4*) were significantly promoted after *sinlrc3* interference ($P < 0.05$, Fig. 4D and G). There was no difference in the expression levels of *zo-1* and *occludin* in the short-term experiment ($P > 0.05$, Fig. 4E). However,

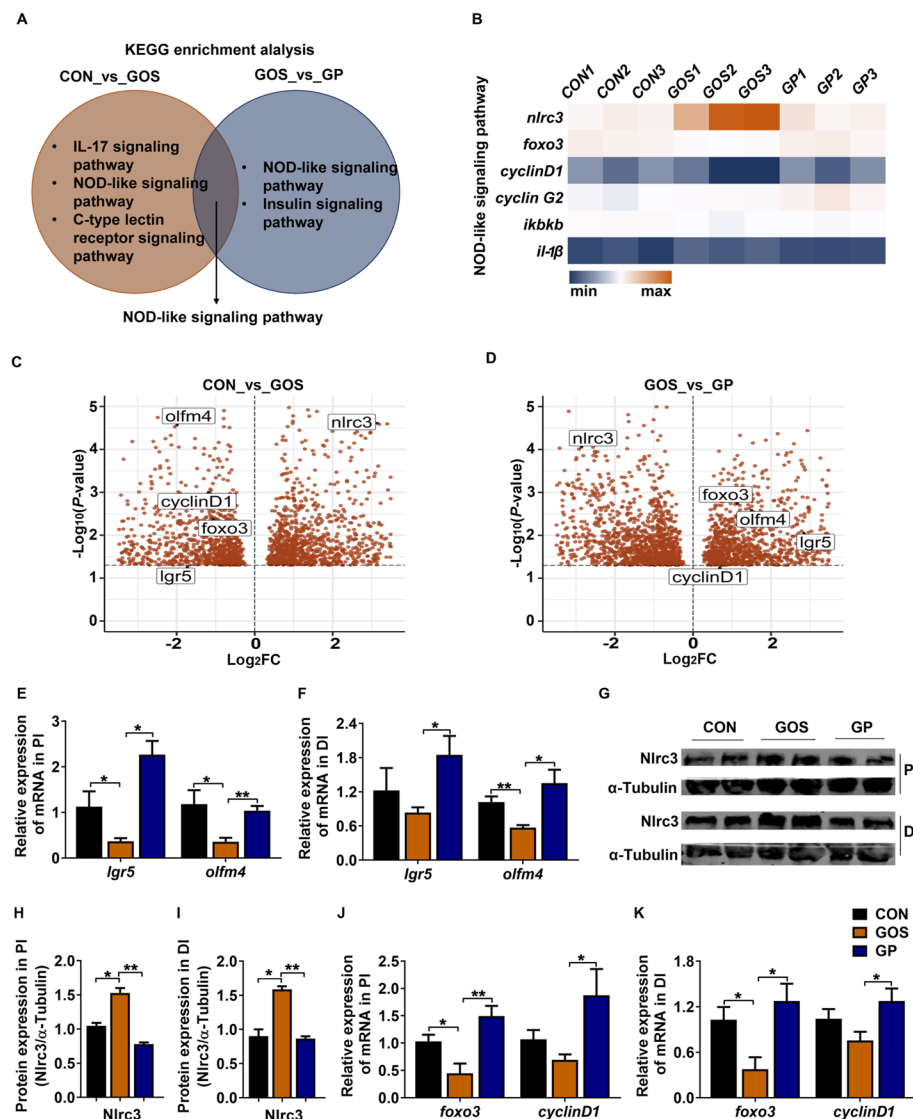


Fig. 3 Addition of *P. pentosaceus* YC inhibited Nlr3 and promoted the gene expression of ISC markers. **A** KEGG enrichment analysis; **B** Heatmap of genes of NOD-like signaling pathway; **C** and **D** Volcano plot of DEGs in the compared groups ($n=3$). **E** and **F** The relative gene expression of ISC markers (*lgr5* and *olfm4*) in PI and DI; **G** The protein expression of Nlr3 in PI and DI; **H** and **I** The quantification of the protein expression of Nlr3 in PI and DI; **J** and **K** The relative gene expression of *foxo3* and *cyclinD1* in PI and DI ($n=6$). Data are represented as mean \pm SEM. Asterisk refers to the significant difference (ANOVA with Tukey's test; * $P < 0.05$, ** $P < 0.01$). CON, control diet; GOS, gossypol diet; GP, gossypol diet supplemented with *P. pentosaceus* YC; FC, fold change; *lgr5*, leucine-rich repeat-containing G protein-coupled receptor 5; *olfm4*, olfactomedin 4; *nlr3*, NLR family CARD domain containing 3; *foxo3*, forkhead box O3; *ikkb*, inhibitor of nuclear factor kappa B kinase; *il-1β*, interleukin-1β; PI, proximal intestine; DI, distal intestine

the expression level of *zo-1* was significantly higher in the long-term experiment ($P < 0.05$, Fig. 4H). These results indicated that the inhibition of *nlr3* had a time-delay effect on promoting the expression of *zo-1* compared with the effect on ISC markers expression.

Addition of *P. pentosaceus* YC altered the composition of gut microbiota

16S rRNA sequencing was conducted to detect whether addition of *P. pentosaceus* YC altered gut microbiota

composition. The abundance of *Pediococcus* was significantly increased in GP group, indicating the successful colonization of *P. pentosaceus* YC in fish gut ($P < 0.05$, Fig. 5A). Dietary *P. pentosaceus* YC had no significant effects on Chao1 (characterized abundance) and Shannon (characterized diversity) indexes ($P > 0.05$, Fig. 5B and C), but significantly increased Faith_pd (characterized phylogenetic diversity) index ($P < 0.05$, Fig. 5D). Addition of *P. pentosaceus* YC recovered the composition of gut microbiota similar to that of the CON group (PCo1 and PCo2

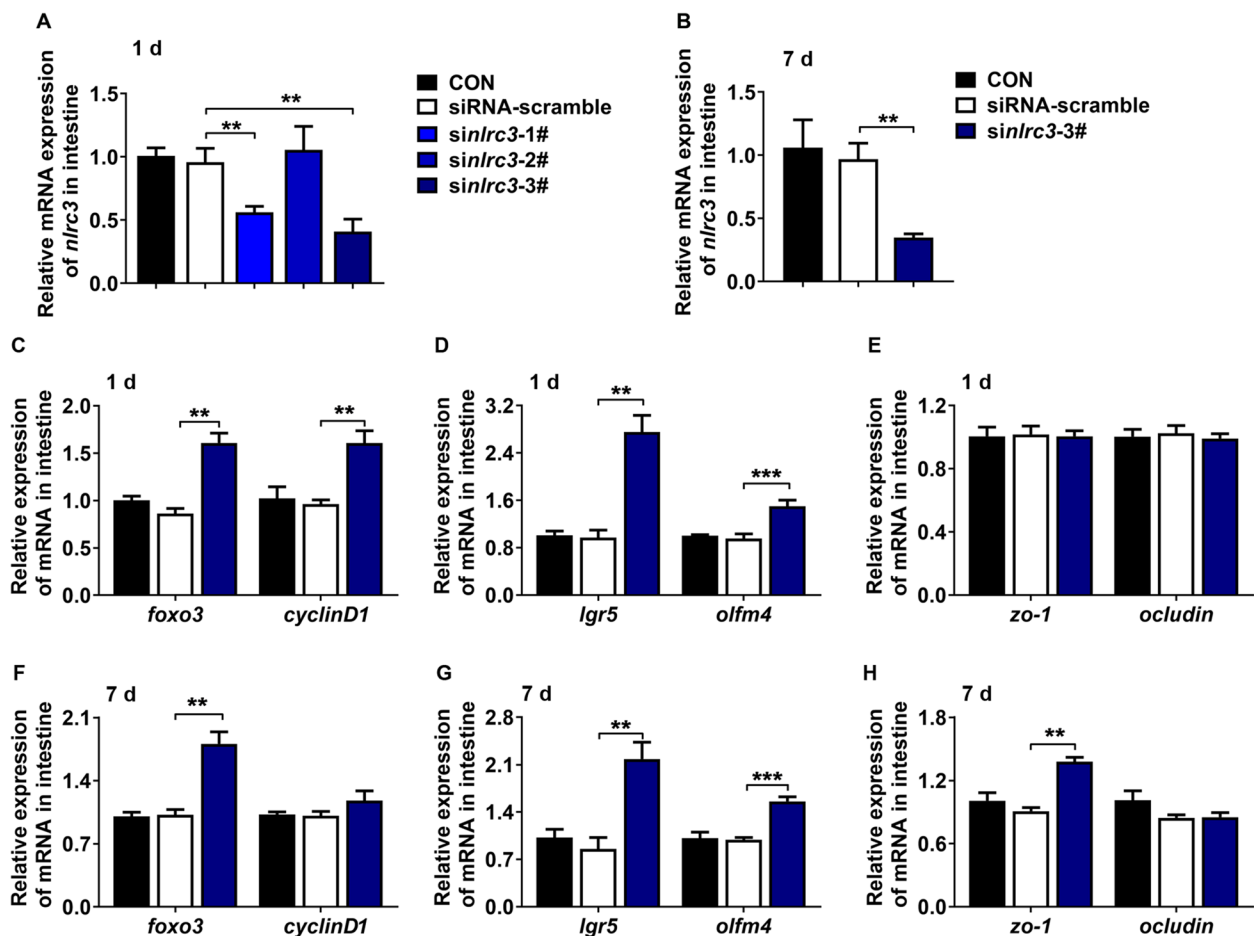


Fig. 4 Nlr3 was the key factor to protect gut barrier integrity. **A** In vivo *sinlrc3* interference for 1 d; **B** In vivo *sinlrc3* interference for 7 d; **C** and **F** The relative gene expression of *foxo3* and *cyclinD1* in the short-term and long-term experiments; **D** and **G** The relative gene expression of *lgr5* and *olfm4* in the short-term and long-term experiments; **E** and **H** The relative gene expression of *zo-1* and *ocludin* in the short-term and long-term experiments ($n = 5$). Data are represented as mean \pm SEM. Significant difference compared with siRNA-scramble group (Student's *t*-test; ** $P < 0.01$, *** $P < 0.001$). CON, control; *nlrc3*, NLR family CARD domain containing 3; *foxo3*, forkhead box O3; *lgr5*, leucine-rich repeat-containing G protein-coupled receptor 5; *olfm4*, olfactomedin 4; *zo-1*, zona occludens 1

were 22.5% and 17.9%, Fig. 5E). LEfSe analysis indicated that Actinobacteria and Nocardioideae were dominant in GOS group, and Pseudonocardiaceae, Bacillaceae and *Pediococcus* were predominant in GP group (Fig. 5F). Proteobacteria, Actinobacteria, Firmicutes, Fusobacteria, and Bacteroidetes were the major phyla across all groups, and addition of *P. pentosaceus* YC increased the abundance of Firmicutes, Fusobacteria, Bacteroidetes, but decreased the abundance of Actinobacteria at the phylum level (Fig. 5G). *Rhizobiales*, *Nocardioideae*, *Cetobacterium*, and *Lactobacillus* were the dominant genera in all three groups, and addition of *P. pentosaceus* YC increased the abundance of *Lactobacillus*, *Cetobacterium*, *Bacteroides*, and decreased the abundance of *Nocardioideae* and *Legionella*

at the genus level (Fig. 5H). Collectively, addition of *P. pentosaceus* YC altered the intestinal microbial composition.

Addition of *P. pentosaceus* YC increased the propionate content in gut

Considering that addition of *P. pentosaceus* YC altered the intestinal microbiota composition, we detected the content of microbial derived acetate, propionate, butyrate, and lactate in the intestinal contents. Butyrate was too low to be detected and there were no notably changes in the levels of lactate and acetate among three groups ($P > 0.05$, Fig. 6A and B). A significant decrease of propionate was observed in GOS group, and addition of *P. pentosaceus* YC restored the level of propionate in GP group ($P < 0.05$,

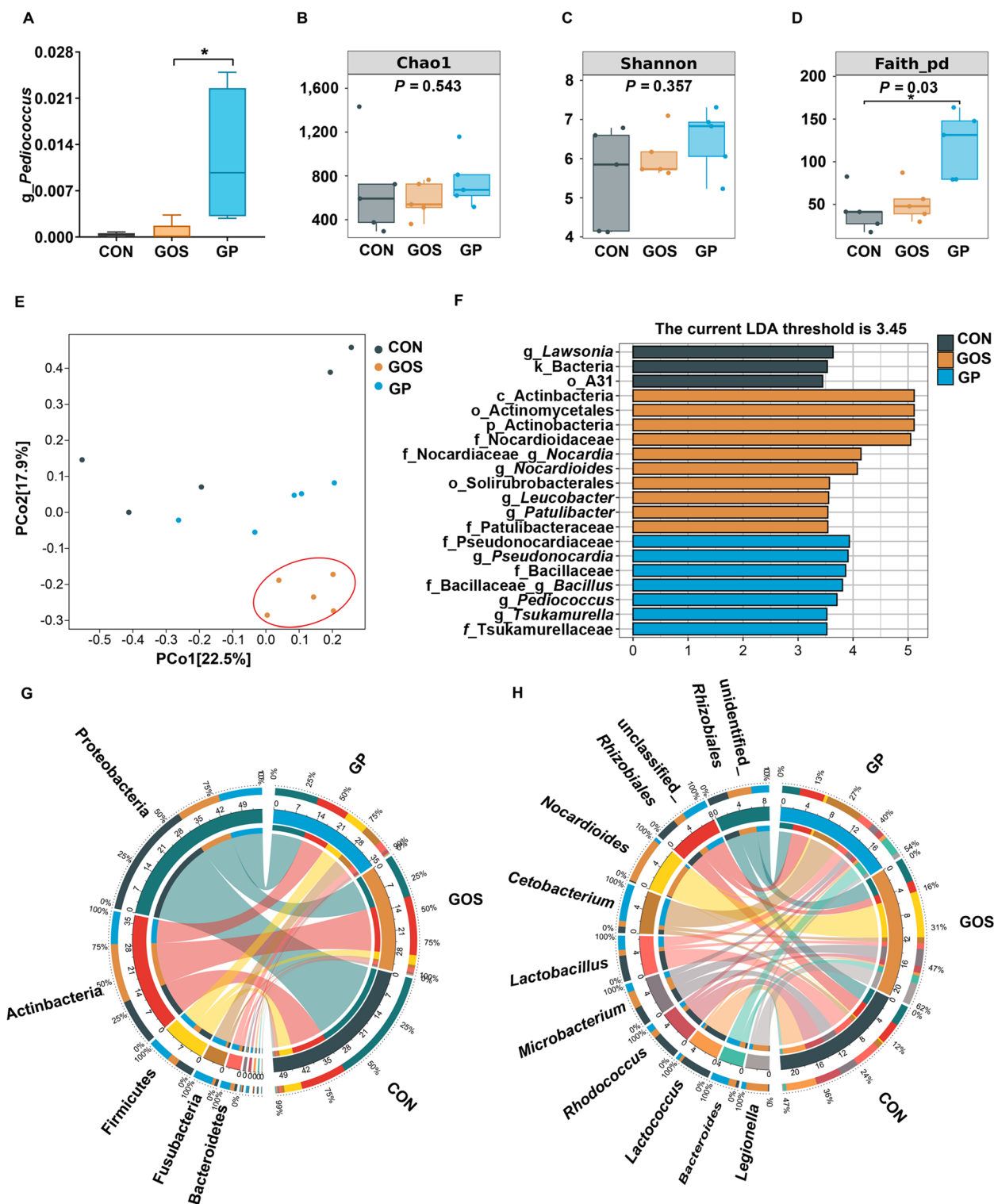


Fig. 5 Addition of *P. pentosaceus* YC altered the composition of gut microbiota. **A** The relative abundance of *Pedfococcus*; **B** Chao1 index; **C** Shannon index; **D** Faith_pd index; **E** PCoA analysis; **F** LefSe analysis; **G** Circos analysis in the level of phylum; **H** Circos analysis in the level of genus ($n=5$). Data are represented as mean \pm SEM. Significant difference of the relative abundance of *Pedfococcus* compared with GOS group (ANOVA with Tukey's test; $*P < 0.05$) and significant difference of Faith_pd (Kruskal-Wallis test; $*P < 0.05$). CON, control diet; GOS, gossypol diet; GP, gossypol diet supplemented with *P. pentosaceus* YC; PCoA, principal coordinate analysis; LDA, laser diffraction analysis

Fig. 6C). Moreover, the expression levels of free fatty acids receptor 2 (*ffar2*, also known as G protein-coupled receptor (*GPR43*)) and *ffar3* (also known as *GPR41*) increased remarkably in the PI and DI after *P. pentosaceus* YC treatment ($P < 0.05$, Fig. 6D and E). In conclusion, addition of *P. pentosaceus* YC increased intestinal propionate content and upregulated the expression of *ffar2* and *ffar3*.

Propionate stimulated wound healing in vitro

The wound-healing assay of Caco-2 cells was conducted to detect the reparative function of propionate. Results revealed that gossypol suppressed the wound healing, but supplementation of sodium propionate strikingly accelerated the healing of wound ($P < 0.05$, Fig. 7A and B). We further detected the above mentioned differentially expressed genes on the Caco-2 cells. Here, we found that *lgr5* had a significantly higher expression after addition of sodium propionate compared to the GOS group, which indicated that propionate might enhance stem cell proliferation during the healing process ($P < 0.05$, Fig. 7C). Furthermore, we examined the expression of *ffar2* and *ffar3*, and found these two genes were significantly upregulated in sodium propionate treatment ($P < 0.05$, Fig. 7D and E). The expression of *nrc3* was dramatically increased in GOS group, and notably decreased by sodium propionate administration ($P < 0.05$, Fig. 7F). These results indicated that propionate inhibited *nrc3* expression, promoted

lgr5 expression, and improved the wound healing of Caco-2 cells.

Discussion

Dietary components and xenobiotics have the adverse effects on the intestinal health [46–48]. Gossypol, a toxic compound contained in CSM, has detrimental effects on the growth condition, intestinal immunity and barrier integrity in various animals, how to decrease the deleterious effects of gossypol residue remains to be explored [13, 17, 19–22]. Probiotics have the potential to promote the growth condition and repair the gut barrier, and concomitantly, intestinal microbiota is involved [34, 36, 49–51]. The present research revealed that the weight gain, specific growth rate and final body length were significantly augmented after the addition of *P. pentosaceus* YC, suggesting its ability to restore the growth retardation caused by gossypol in Nile tilapia. The increased growth may be attributed to the repair of gut barrier, as intestinal structure integrity is indispensable for the absorption of nutrients and resisting of pathogens [52]. Wang et al. [17] reported that dietary gossypol resulted in the loose arrangement of enterocyte and epithelial sloughing to damage the structure of intestinal epithelial cells in grass carp (*Ctenopharyngodon idella*), but there is no effective strategy to reduce the negative effect of

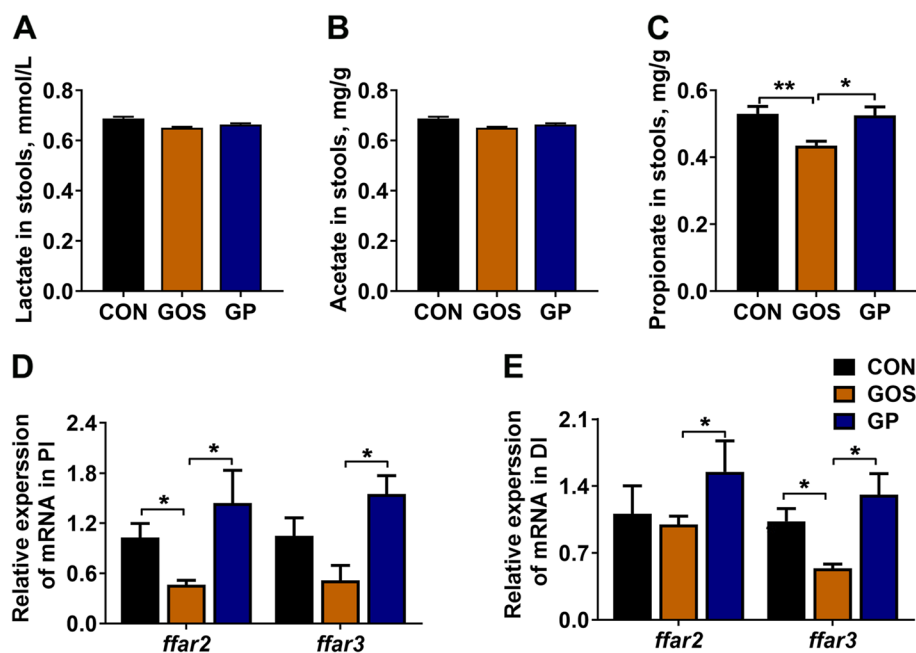


Fig. 6 Addition of *P. pentosaceus* YC induced the accumulation of gut propionate. **A** The levels of lactate in the intestinal contents; **B** The levels of acetate in the intestinal contents; **C** The levels of propionate in the intestinal contents; **D** and **E** The relative genes expression of *ffar2* and *ffar3* in PI and DI ($n = 6$). Data are represented as mean \pm SEM. Asterisk refers to the significant difference (ANOVA with Tukey's test; * $P < 0.05$, ** $P < 0.01$). CON, control diet; GOS, gossypol diet; GP, gossypol diet supplemented with *P. pentosaceus* YC; *ffar*, free fatty acid receptor; PI, proximal intestine; DI, distal intestine

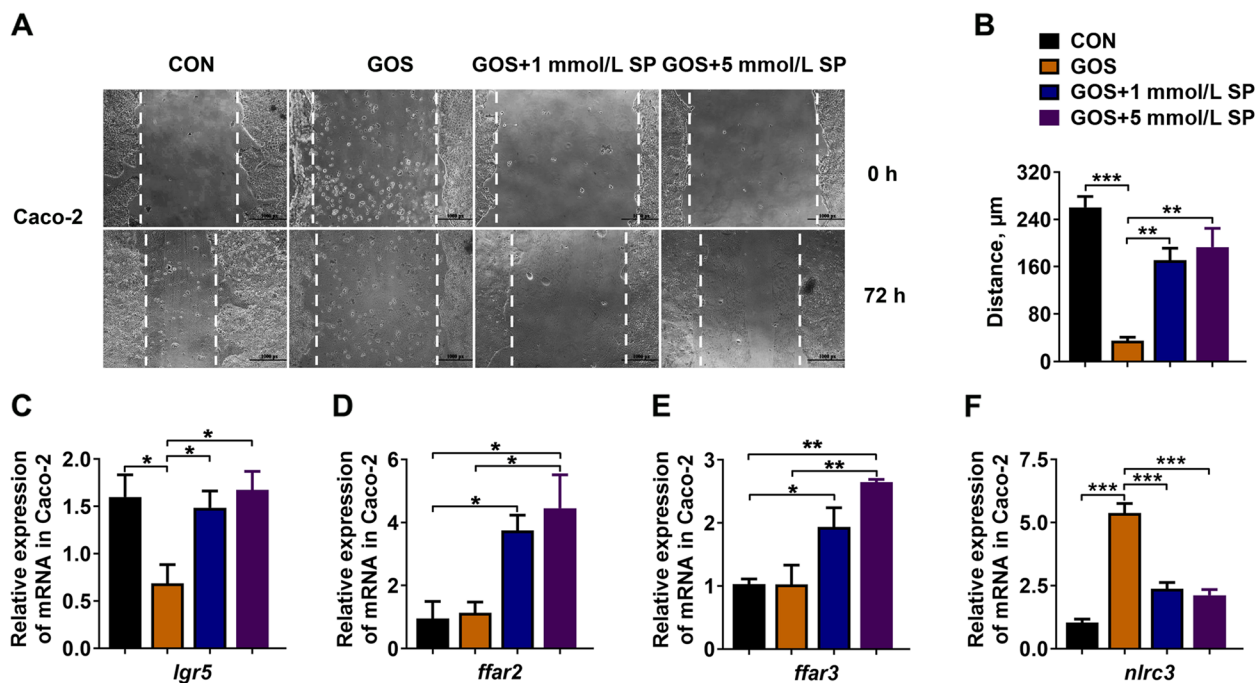


Fig. 7 Propionate improved the wound healing of Caco-2 cells in vitro. **A** Representative phase contrast images of Caco-2 cells, scale bar=1,000 px (1 px=4.23 µm); **B** Quantification of average migration distance; **C–F** The relative gene expression of *lgr5*, *ffar2*, *ffar3* and *nlrc3* in Caco-2 cells ($n=3$). Asterisk refers to the significant difference (ANOVA with Tukey's test; * $P<0.05$, ** $P<0.01$, *** $P<0.001$). CON, control; GOS, gossypol; SP, sodium propionate; *lgr5*, leucine-rich repeat-containing G protein-coupled receptor 5; *ffar*, free fatty acid receptor; *nlrc3*, NLR family CARD domain containing 3

gossypol. Our previous study in Nile tilapia proved that the disruption of intestinal microbial homeostasis was the reason for gossypol to exacerbate gut barrier injury [21]. And in the present study, we found that addition of *P. pentosaceus* could improve the intestinal structure and integrity when fish were exposed to gossypol.

ISC proliferation is fundamental to sustaining gut barrier integrity by governing the rapid renewal of intestinal epithelium, particularly in response to gut barrier injury [32, 34, 53]. Several signaling pathways including NLR, Wnt, bone morphogenetic protein (BMP) and Notch signals have been documented to regulate ISC proliferation [32]. Here, the RNAseq analysis inspired us to focus on the Nlrc3 (also named CLR16.2 and Nod3), a molecular belonging to NLRs family [54]. NOD1 and NOD2 in the NLRs family are capable of regulating ISC proliferation [55–57]. However, the link between Nlrc3 and ISC proliferation has not been explored. Research has discovered that a deficiency of NLRC3 spurred cell proliferation in wound and hastened the healing of murine cutaneous wound [58]. Correspondingly, the results of the feeding trial substantiated that the expression of Nlrc3 had a negative correlation with the expression of ISC markers, *lgr5* and *olfn4*, and the siRNA interference experiment

indicated that inhibition of Nlrc3 could stimulate the expression of these genes, potentially implying ISC proliferation. *Foxo3* and *cyclinD1* were two downstream genes of *nlrc3* [59], and *cyclinD1* was found to contribute to porcine ISC proliferation [35]. In this study, the expression levels of *foxo3* and *cyclinD1* were up-regulated when *nlrc3* was inhibited, suggesting that the effect of *nlrc3* on *foxo3* and *cyclinD1* was conserved in different animals. The proliferated ISCs could move up and divide into epithelial cells to replace the damaged cells in the villi [60]. We also found the expression of *si* (a marker of terminal differentiation in enterocytes) and *villin* (enterocytes marker) increased when *P. pentosaceus* YC was added (Fig. S1), suggesting that the addition of *P. pentosaceus* YC may also influence the differentiation to enterocytes, yet this requires more validation. Furthermore, it has been revealed that mice lacking NLRC3 were predisposed to cancer due to hyperproliferation [59], so we identified whether addition of *P. pentosaceus* YC with standard diet caused harmful effect to the host. The results showed that addition of *P. pentosaceus* YC did not influence the growth performance or intestinal barrier function (Fig. S2), indicating *P. pentosaceus* YC did not induce the excessive proliferation under the normal physiological condition of fish.

The intestinal microbiota and the derived metabolites can initiate signals of hosts to maintain the gut barrier integrity [61, 62]. Previous study has demonstrated that addition of *P. pentosaceus* altered the gut microbiota composition in mice and zebrafish [29–31, 38]. Consistently, *P. pentosaceus* YC administration raised the abundance of Firmicutes, Fusobacteria, Bacteroidetes phyla and *Lactobacillus*, *Cetobacterium*, and *Bacteroides* genera. These bacteria are capable of effectively producing SCFAs, which can help to repair intestinal barrier damage [63–65]. The metabolites analysis further indicated that the addition of *P. pentosaceus* YC increased the level of propionate significantly. Unlike the beneficial effect of acetate and butyrate in maintaining intestinal barrier [66, 67], the effect of propionate on gut barrier was inconsistent [68, 69]. It has been found that propionate supplementation in high-fat diet induced intestine damage in zebrafish [68], but sodium propionate supplementation in the diet with high soybean meal promoted the growth performance of turbot and enhanced the expression of intestinal tight junction proteins [69]. In our study, exogenous addition of sodium propionate promoted wound healing of Caco-2 cells, insinuating the reparative effect on gut barrier integrity of propionate with the presence of gossypol.

Caco-2 cells line was used because it has a classical intestinal crypt stem cell-like population and can differentiate into intestinal epithelial-like cells, which is an ideal model to research the connection between ISCs and intestinal epithelium [70, 71]. With the addition of sodium propionate, we discovered a high expression of LGR5 [70], a marker of the classic intestinal crypt stem cell-like population of Caco-2 cells, indicating stem cell proliferation. GPR41 and GPR43 are known to mediate propionate to promote murine intestinal stem cell proliferation [72]. Moreover, SCFAs has been proved to inhibit NLRs by activating GPRs [73]. Here, propionate increased *ffar2/ffar3* expression and decreased *nlrc3* expression in vitro and in vivo, indicating propionate may inhibit Nlrc3 through GPRs. Taken together, addition of *P. pentosaceus* YC increased the level of gut microbiota-derived propionate and repaired gossypol-induced intestinal barrier injury in Nile tilapia.

Conclusions

In conclusion, the present study established that *P. pentosaceus* YC had the protective effect on repairing gossypol-induced intestinal barrier injury. Addition of *P. pentosaceus* YC altered the gut microbiota composition and increased intestinal propionate to inhibit Nlrc3, up-regulated the genes of ISC proliferation markers and repaired intestinal barrier injury. This study provides a potential strategy for gossypol-induced gut barrier injury, which will also benefit the application of CSM in the future.

Abbreviations

ANOVA	One-way analysis of variance
BCA	Bicinchoninic acid
BMP	Bone morphogenetic protein
CARD	Caspase recruitment domain
CF	Condition factor
CFU	Colony-forming unit
CON	Control diet
CSM	Cottonseed meal
DEG	Differentially expressed gene
DI	Distal intestine
ef1 α	Elongation factor 1 alpha
ELISA	Enzyme-linked immunosorbent assays
FBW	Final body weight
FC	Fold change
ffar	Free fatty acid receptor
FM	Fish meal
foxo3	Forkhead box O3
GC-MS	Gas chromatography-mass spectrometry
GOS	Gossypol diet
GP	Gossypol diet supplemented with <i>P. pentosaceus</i> YC
H&E	Hematoxylin and eosin
HSI	Hepatosomatic index
IBW	Initial body weight
il-1 β	Interleukin-1 β
ISC	Intestinal stem cell
ikbkb	Inhibitor of nuclear factor kappa B kinase
KEGG	Kyoto Encyclopedia of Genes and Genomes
LDA	Laser diffraction analysis
LEfSe	Linear discriminant analysis effect size
Lgr5	Leucine-rich repeat-containing G-protein coupled receptor 5
LPS	Lipopolysaccharide
MFI	Mesenteric fat index
MRS	Man Rogosa Sharpe
Nlrc3	NLR family CARD domain containing 3
NLR	NOD-like receptors
Olfm4	Olfactomedin 4
PBS	Phosphate buffered saline
PCoA	Principal coordinate analysis
PI	Proximal intestine
PMSF	Phenylmethylsulfonyl fluoride
qPCR	Quantitative PCR
RIPA	Radioimmunoprecipitation assay
SBM	Soybean meal
SCFA	Short chain fatty acid
SDS	Sodium dodecyl sulfate
SDS-PAGE	Sodium dodecyl sulfate polyacrylamide gel electrophoresis
SEM	Standard error of mean
SGR	Specific growth rate
SP	Sodium propionate
TEER	Transepithelial electrical resistance
WG	Weight gain
zo-1	Zona occludens 1

Supplementary Information

The online version contains supplementary material available at <https://doi.org/10.1186/s40104-024-01011-w>.

Additional file 1: Table S1. Ingredient formulation and proximate composition of the experimental diets (dry matter basis). **Table S2.** Primer pair sequences and product size of the genes used for qPCR. **Table S3.** *nlrc3* siRNA information. **Fig. S1.** Addition of *P. pentosaceus* YC promoted the gene expression of enterocytes. **Fig. S2.** Administration of *P. pentosaceus* YC have no effect on Nile tilapia fed with the control diet. **Supplementary methods.** Animal experiments, proximate composition analysis, high liquid chromatography analysis of gossypol.

Acknowledgments

We extend our thanks to the technical support from the instruments sharing platform of school of life sciences, East China Normal University.

Authors' contributions

MLZ and FFD conceived the study and designed the experiments. FFD and NNZ carried out the experiments and analyzed the data. FFD wrote the manuscript. MLZ and YL revised the manuscript. FFD, NNZ, YL, TW, WJL, FQ, ZYD, MLZ contributed material preparation, methodology, and supervision. All authors read and approved the final manuscript.

Funding

This study was supported by the Provincial Science and Technology Innovative Program for Carbon Peak and Carbon neutrality of Jiangsu of China (BE2022422); National Natural Science Foundation of China (32373145).

Availability of data and materials

All data supporting our findings are included in the manuscript.

Declarations

Ethics approval and consent to participate

All experiments were performed according to the Guidance of the Care and Use of Laboratory Animals in China and approved by the Committee on the Ethics of Animal Experiments of East China Normal University (No. F20201002).

Consent for publication

Not applicable.

Competing interests

The authors declare no competing interests.

Author details

¹Laboratory of Aquaculture Nutrition and Environmental Health (LANEH), School of Life Sciences, East China Normal University, Shanghai 200241, China.

Received: 1 December 2023 Accepted: 6 February 2024

Published online: 07 April 2024

References

- Citi S. Intestinal barriers protect against disease. *Science*. 2018;359(6380):1097–8. <https://doi.org/10.1126/science.aat0835>.
- Chelakkot C, Ghim J, Ryu SH. Mechanisms regulating intestinal barrier integrity and its pathological implications. *Exp Mol Med*. 2018;50:1–9. <https://doi.org/10.1038/s12276-018-0126-x>.
- Luissint AC, Parkos CA, Nusrat A. Inflammation and the intestinal barrier: leukocyte-epithelial cell interactions, cell junction remodeling, and mucosal repair. *Gastroenterol*. 2016;151(4):616–32. <https://doi.org/10.1053/j.gastro.2016.07.008>.
- Fang Q, Yu L, Tian F, Zhang H, Chen W, Zhai Q. Effects of dietary irritants on intestinal homeostasis and the intervention strategies. *Food Chem*. 2023;409:135280–93. <https://doi.org/10.1016/j.foodchem.2022.135280>.
- Di Tommaso N, Gasbarrini A, Ponziani FR. Intestinal barrier in human health and disease. *Int J Environ Res Public Health*. 2021;18(23):12836–59. <https://doi.org/10.3390/ijerph182312836>.
- Vancamelbeke M, Vermeire S. The intestinal barrier: a fundamental role in health and disease. *Expert Rev Gastroenterol Hepatol*. 2017;11(9):821–34. <https://doi.org/10.1080/17474124.2017.1343143>.
- McCole DF. IBD candidate genes and intestinal barrier regulation. *Inflamm Bowel Dis*. 2014;20(10):1829–49. <https://doi.org/10.1097/mib.000000000000090>.
- Chopyk DM, Grakoui A. Contribution of the intestinal microbiome and gut barrier to hepatic disorders. *Gastroenterol*. 2020;159(3):849–63. <https://doi.org/10.1053/j.gastro.2020.04.077>.
- Pabst O, Hornef MW, Schaap FG, Cerovic V, Clavel T, Bruns T. Gut-liver axis: barriers and functional circuits. *Nat Rev Gastroenterol Hepatol*. 2023;20(7):447–61. <https://doi.org/10.1038/s41575-023-00771-6>.
- Travier L, Alonso M, Andronico A, Hafner L, Disson O, Lledo PM, et al. Neonatal susceptibility to meningitis results from the immaturity of epithelial barriers and gut microbiota. *Cell Rep*. 2021;35(13):109319–41. <https://doi.org/10.1016/j.celrep.2021.109319>.
- Zhou Q, Verne GN. Intestinal hyperpermeability: a gateway to multi-organ failure? *J Clin Invest*. 2018;128(11):4764–6. <https://doi.org/10.1172/jci124366>.
- Montoya-Camacho N, Marquez-Ríos E, Castillo-Yáez FJ, JLC L, López-Elías JA, Ruiz-Cruz S, et al. Advances in the use of alternative protein sources for tilapia feeding. *Rev Aquacult*. 2019;11(3):515–26. <https://doi.org/10.1111/raq.12243>.
- Yu J, Wang ZY, Yang HM, Xu L, Wan XL. Effects of cottonseed meal on growth performance, small intestinal morphology, digestive enzyme activities, and serum biochemical parameters of geese. *Poult Sci*. 2019;98(5):2066–71. <https://doi.org/10.3382/ps/pey553>.
- Bu XY, Chen AJ, Lian XQ, Chen FY, Zhang Y, Muhammad I, et al. An evaluation of replacing fish meal with cottonseed meal in the diet of juvenile USSURI catfish *Pseudobagrus ussuriensis*: growth, antioxidant capacity, non-specific immunity and resistance to *Aeromonas hydrophila*. *Aquaculture*. 2017;479:829–37. <https://doi.org/10.1016/j.aquaculture.2017.07.032>.
- Li MH, Robinson EH. Use of cottonseed meal in aquatic animal diets: a review. *N Am J Aquac*. 2006;68(1):14–22. <https://doi.org/10.1577/A05-028.1>.
- Delgado E, Valles-Rosales DJ, Flores NC, Jáquez DR. Evaluation of fish oil content and cottonseed meal with ultralow gossypol content on the functional properties of an extruded shrimp feed. *Aquaculture Rep*. 2021;19(4):100588–94. <https://doi.org/10.1016/j.aqrep.2021.100588>.
- Wang KZ, Feng L, Jiang WD, Wu P, Liu Y, Jiang J, et al. Dietary gossypol reduced intestinal immunity and aggravated inflammation in on-growing grass carp (*Ctenopharyngodon idella*). *Fish Shellfish Immunol*. 2019;86:814–31. <https://doi.org/10.1016/j.fsi.2018.12.014>.
- Yin B, Liu H, Tan B, Dong X, Chi S, Yang Q, et al. Preliminary study of mechanisms of intestinal inflammation induced by plant proteins in juvenile hybrid groupers (*♀Epinephelus fuscoguttatus* × *♂E. lanceolatus*). *Fish Shellfish Immunol*. 2020;106:341–56. <https://doi.org/10.1016/j.fsi.2020.07.026>.
- Irm M, Ye B, Wu X, Geng L, Cai Q, Zhang L, et al. Assessment of conventional and low gossypol cottonseed meal as alternative protein sources in low-fishmeal diets of hybrid grouper (*Epinephelus fuscoguttatus* ♀ × *Epinephelus lanceolatus* ♂): growth, feed utilization, gut histology, and immunity. *Animals (Basel)*. 2022;12(15):1906–22. <https://doi.org/10.3390/ani12151906>.
- Jazi V, Boldaji F, Dastar B, Hashemi SR, Ashayerizadeh A. Effects of fermented cottonseed meal on the growth performance, gastrointestinal microflora population and small intestinal morphology in broiler chickens. *Br Poult Sci*. 2017;58(4):402–8. <https://doi.org/10.1080/00071668.2017.1315051>.
- Li WJ, Zhang L, Wu HX, Li M, Wang T, Zhang WB, et al. Intestinal microbiota mediates gossypol-induced intestinal inflammation, oxidative stress, and apoptosis in fish. *J Agric Food Chem*. 2022;70(22):6688–97. <https://doi.org/10.1021/acs.jafc.2c01263>.
- Li WJ, Wu HX, Zhang L, Li M, Wang T, Shan CJ, et al. Effects of replacing soybean meal protein with cottonseed protein concentrate on the growth condition and intestinal health of Nile tilapia (*Oreochromis niloticus*). *Aquac Nutr*. 2021;27(6):2436–47. <https://doi.org/10.1111/anu.13375>.
- Zhou M, Zhang C, Wu Y, Tang Y. Metabolic engineering of gossypol in cotton. *Appl Microbiol Biotechnol*. 2013;97(14):6159–65. <https://doi.org/10.1007/s00253-013-5032-5>.
- Chen S, Lin Y, Shi H, Miao L, Liu B, Ge X. Dietary ferulic acid supplementation improved cottonseed meal-based diet utilization by enhancing intestinal physical barrier function and liver antioxidant capacity in grass carp (*Ctenopharyngodon idellus*). *Front Physiol*. 2022;13:922037–52. <https://doi.org/10.3389/fphys.2022.922037>.
- Lim SJ, Kim SS, Pham MA, Song JW, Cha JH, Kim JD, et al. Effects of fermented cottonseed and soybean meal with phytase supplementation on gossypol degradation, phosphorus availability, and growth performance of olive flounder (*Paralichthys olivaceus*). *Fish Aquat Sci*. 2010;13(4):284–93. <https://doi.org/10.5657/fas.2010.13.4.284>.
- Lim SJ, Lee KJ. Supplemental iron and phosphorus increase dietary inclusion of cottonseed and soybean meal in olive flounder (*Paralichthys*

- olivaceus*). *Aquacult Nutr.* 2008;14(5):423–30. <https://doi.org/10.1111/j.1365-2095.2007.00546.x>.
27. Hoseinifar SH, Sun YZ, Wang A, Zhou Z. Probiotics as means of diseases control in aquaculture, a review of current knowledge and future perspectives. *Front Microbiol.* 2018;9:2429–47. <https://doi.org/10.3389/fmicb.2018.02429>.
 28. Liao SF, Nyachoti M. Using probiotics to improve swine gut health and nutrient utilization. *Anim Nutr.* 2017;3(4):331–43. <https://doi.org/10.1016/j.aninu.2017.06.007>.
 29. Dong F, Xiao F, Li X, Li Y, Wang X, Yu G, et al. *Pediococcus pentosaceus* CECT 8330 protects DSS-induced colitis and regulates the intestinal microbiota and immune responses in mice. *J Transl Med.* 2022;20(1):33–49. <https://doi.org/10.1186/s12967-022-03235-8>.
 30. Hao L, Cheng Y, Su W, Wang C, Lu Z, Jin M, et al. *Pediococcus pentosaceus* ZJUAF-4 relieves oxidative stress and restores the gut microbiota in diquat-induced intestinal injury. *Appl Microbiol Biotechnol.* 2021;105(4):1657–68. <https://doi.org/10.1007/s00253-021-11111-6>.
 31. Liu Y, Zhu D, Liu J, Sun X, Gao F, Duan H, et al. *Pediococcus pentosaceus* PR-1 modulates high-fat-diet-induced alterations in gut microbiota, inflammation, and lipid metabolism in zebrafish. *Front Nutr.* 2023;10:1087703–17. <https://doi.org/10.3389/fnut.2023.1087703>.
 32. Ma N, Chen X, Johnston LJ, Ma X. Gut microbiota-stem cell niche crosstalk: A new territory for maintaining intestinal homeostasis. *iMeta.* 2022;1(4):e54. <https://doi.org/10.1002/imt2.54>.
 33. Barker N, van Es JH, Kuipers J, Kujala P, van den Born M, Cozijnsen M, et al. Identification of stem cells in small intestine and colon by marker gene Lgr5. *Nature.* 2007;449(7165):1003–7. <https://doi.org/10.1038/nature06196>.
 34. Wu H, Xie S, Miao J, Li Y, Wang Z, Wang M, et al. *Lactobacillus reuteri* maintains intestinal epithelial regeneration and repairs damaged intestinal mucosa. *Gut Microbes.* 2020;11(4):997–1014. <https://doi.org/10.1080/19490976.2020.1734423>.
 35. Qin YC, Zhou JY, Zhu M, Zan GX, Gao CQ, Yan HC, et al. L-glutamate requires beta-catenin signalling through Frizzled7 to stimulate porcine intestinal stem cell expansion. *Cell Mol Life Sci.* 2022;79(10):523–36. <https://doi.org/10.1007/s00018-022-04545-2>.
 36. Chen L, Li S, Peng C, Gui Q, Li J, Xu Z, et al. *Lactobacillus rhamnosus* GG promotes recovery of the colon barrier in septic mice through accelerating ISCs regeneration. *Nutrients.* 2023;15(3):672. <https://doi.org/10.3390/nu15030672>.
 37. Luo Y, Li M, Wang T, Zhou NN, Qiao F, Du ZY, et al. *Bacillus cereus* alters bile acid composition and alleviates high-carbohydrate diet-induced hepatic lipid accumulation in Nile Tilapia (*Oreochromis niloticus*). *J Agric Food Chem.* 2023;71(12):4825–36. <https://doi.org/10.1021/acs.jafc.2c07945>.
 38. Shan CJ, Li M, Liu Z, Xu R, Qiao F, Du ZY, et al. *Pediococcus pentosaceus* enhances host resistance against pathogen by increasing IL-1 β production: understanding probiotic effectiveness and administration duration. *Front Immunol.* 2021;12:766401–14. <https://doi.org/10.3389/fimmu.2021.766401>.
 39. Zhang ML, Li M, Sheng Y, Tan F, Chen L, Cann I, et al. *Citrobacter* species increase energy harvest by modulating intestinal microbiota in fish: non-dominant species play important functions. *mSystems.* 2020;5(3):e00303–20. <https://doi.org/10.1128/mSystems.00303-20>.
 40. Limbu SM, Ma Q, Zhang ML, Du ZY. High fat diet worsens the adverse effects of antibiotic on intestinal health in juvenile Nile tilapia (*Oreochromis niloticus*). *Sci Total Environ.* 2019;680:169–80. <https://doi.org/10.1016/j.scitotenv.2019.05.067>.
 41. den Besten G, van Eunen K, Groen AK, Venema K, Reijngoud DJ, Bakker BM. The role of short-chain fatty acids in the interplay between diet, gut microbiota, and host energy metabolism. *J Lipid Res.* 2013;54(9):2325–40. <https://doi.org/10.1194/jlr.R036012>.
 42. Srinivasan B, Kolli AR, Esch MB, Abaci HE, Shuler ML, Hickman JJ. TEER measurement techniques for in vitro barrier model systems. *J Lab Autom.* 2015;20(2):107–26. <https://doi.org/10.1177/2211068214561025>.
 43. Liu Q, Tian H, Kang Y, Tian Y, Li L, Kang X, et al. Probiotics alleviate autoimmune hepatitis in mice through modulation of gut microbiota and intestinal permeability. *J Nutr Biochem.* 2021;98:108863–75. <https://doi.org/10.1016/j.jnutbio.2021.108863>.
 44. Garcia-Hernandez V, Quiros M, Nusrat A. Intestinal epithelial claudins: expression and regulation in homeostasis and inflammation. *Ann NY Acad Sci.* 2017;1397(1):66–79. <https://doi.org/10.1111/nyas.13360>.
 45. Lee SH. Intestinal permeability regulation by tight junction: implication on inflammatory bowel diseases. *Intest Res.* 2015;13(1):11–8. <https://doi.org/10.5217/ir.2015.13.1.11>.
 46. Yang J, Wei H, Zhou Y, Szeto CH, Li C, Lin Y, et al. High-fat diet promotes colorectal tumorigenesis through modulating gut microbiota and metabolites. *Gastroenterol.* 2022;162(1):135–49.e2. <https://doi.org/10.1053/j.gastro.2021.08.041>.
 47. Kwon YH, Banskota S, Wang H, Rossi L, Grondin JA, Syed SA, et al. Chronic exposure to synthetic food colorant Allura red AC promotes susceptibility to experimental colitis via intestinal serotonin in mice. *Nat Commun.* 2022;13:7617–35. <https://doi.org/10.1038/s41467-022-35309-y>.
 48. Xia B, Zhong R, Wu W, Luo C, Meng Q, Gao Q, et al. Mucin O-glycan-microbiota axis orchestrates gut homeostasis in a diarrheal pig model. *Microbiome.* 2022;10:139. <https://doi.org/10.1186/s40168-022-01326-8>.
 49. Geng S, Cheng S, Li Y, Wen Z, Ma X, Jiang X, et al. Faecal microbiota transplantation reduces susceptibility to epithelial injury and modulates tryptophan metabolism of the microbial community in a piglet model. *J Crohns Colitis.* 2018;12(11):1359–74. <https://doi.org/10.1093/ecco-jcc/jjy103>.
 50. Yu L, Zhang L, Duan H, Zhao R, Xiao Y, Guo M, et al. The protection of *Lactiplantibacillus plantarum* CCFM8661 against benzopyrene-induced toxicity via regulation of the gut microbiota. *Front Immunol.* 2021;12:736129–43. <https://doi.org/10.3389/fimmu.2021.736129>.
 51. Sofi MH, Wu Y, Ticer T, Schutt S, Bastian D, Choi HJ, et al. A single strain of *Bacteroides fragilis* protects gut integrity and reduces GVHD. *JCI Insight.* 2021;6(3):e136841–57. <https://doi.org/10.1172/jci.insight.136841>.
 52. Circu ML, Aw TY. Intestinal redox biology and oxidative stress. *Semin Cell Dev Biol.* 2012;23(7):729–37. <https://doi.org/10.1016/j.semcdb.2012.03.014>.
 53. Hou Q, Ye L, Liu H, Huang L, Yang Q, Turner JR, et al. *Lactobacillus* accelerates ISCs regeneration to protect the integrity of intestinal mucosa through activation of STAT3 signaling pathway induced by LPLs secretion of IL-22. *Cell Death Differ.* 2018;25(9):1657–70. <https://doi.org/10.1038/s41418-018-0070-2>.
 54. Kanneganti TD, Lamkanfi M, Núñez G. Intracellular NOD-like receptors in host defense and disease. *Immunity.* 2007;27(4):549–59. <https://doi.org/10.1016/j.immuni.2007.10.002>.
 55. Levy A, Stedman A, Deutsch E, Donnadieu F, Virgin HW, Sansonetti PJ, et al. Innate immune receptor NOD2 mediates LGR5⁺ intestinal stem cell protection against ROS cytotoxicity via mitophagy stimulation. *Proc Natl Acad Sci USA.* 2020;117(4):1994–2003. <https://doi.org/10.1073/pnas.1902788117>.
 56. Schwarzer M, Gautam UK, Makki K, Lambert A, Brabec T, Joly A, et al. Microbe-mediated intestinal NOD2 stimulation improves linear growth of undernourished infant mice. *Science.* 2023;379(6634):826–33. <https://doi.org/10.1126/science.ade9767>.
 57. Fritz JH. Nod-like receptors have a grip on stem cells. *Cell Host Microbe.* 2014;15(6):659–61. <https://doi.org/10.1016/j.chom.2014.05.017>.
 58. Qin Y, Wu K, Zhang Z, Pan R, Lin Z, Zhang W, et al. NLR3 deficiency promotes cutaneous wound healing due to the inhibition of p53 signaling. *Biochim Biophys Acta Mol Basis Dis.* 2022;1868(11):166518–30. <https://doi.org/10.1016/j.bbadis.2022.166518>.
 59. Karki R, Malireddi RKS, Zhu Q, Kanneganti TD. NLR3 regulates cellular proliferation and apoptosis to attenuate the development of colorectal cancer. *Cell Cycle.* 2017;16(13):1243–51. <https://doi.org/10.1080/15384101.2017.1317414>.
 60. Won JH, Choi JS, Jun JI. CCN1 interacts with integrins to regulate intestinal stem cell proliferation and differentiation. *Nat Commun.* 2022;13:3117–33. <https://doi.org/10.1038/s41467-022-30851-1>.
 61. Kayama H, Okumura R, Takeda K. Interaction between the microbiota, epithelia, and immune cells in the intestine. *Annu Rev Immunol.* 2020;38:23–48. <https://doi.org/10.1146/annurev-immunol-070119-115104>.
 62. Ghosh S, Whitley CS, Haribabu B, Jala VR. Regulation of intestinal barrier function by microbial metabolites. *Cell Mol Gastroenterol Hepatol.* 2021;11(5):1463–82. <https://doi.org/10.1016/j.cmg.2021.02.007>.
 63. Zhao T, Yue H, Peng J, Nie Y, Wu L, Li T, et al. Degradation of xylan by human gut *Bacteroides xylanisolvens* XB1A. *Carbohydr Polym.* 2023;315:121005–18. <https://doi.org/10.1016/j.carbpol.2023.121005>.
 64. Liao X, Lan Y, Wang W, Zhang J, Shao R, Yin Z, et al. Vitamin D influences gut microbiota and acetate production in zebrafish (*Danio rerio*) to promote intestinal immunity against invading pathogens. *Gut Microbes.* 2023;15(1):2187575–89. <https://doi.org/10.1080/19490976.2023.2187575>.

65. Zhang M, Li RW, Yang H, Tan Z, Liu F. Recent advances in developing butyrogenic functional foods to promote gut health. *Crit Rev Food Sci Nutr*. 2022;4:1–22. <https://doi.org/10.1080/10408398.2022.2142194>.
66. Wang RX, Lee JS, Campbell EL, Colgan SP. Microbiota-derived butyrate dynamically regulates intestinal homeostasis through regulation of actin-associated protein synaptopodin. *Proc Natl Acad Sci USA*. 2020;117(21):11648–57. <https://doi.org/10.1073/pnas.1917597117>.
67. Deleu S, Machiels K, Raes J, Verbeke K, Vermeire S. Short chain fatty acids and its producing organisms: an overlooked therapy for IBD? *E Bio Med*. 2021;66:103293–306. <https://doi.org/10.1016/j.ebiom.2021.103293>.
68. Ding Q, Zhang Z, Li Y, Liu H, Hao Q, Yang Y, et al. Propionate induces intestinal oxidative stress via Sod2 propionylation in zebrafish. *iScience*. 2021;24(6):102515–40. <https://doi.org/10.1016/j.isci.2021.102515>.
69. Sun H, Zhang J, Wang W, Shao R, Liang S, Xu W, et al. The effects of sodium propionate supplementation in the diet with high soybean meal on growth performance, intestinal health, and immune resistance to bacterial infection in turbot (*Scophthalmus maximus* L.). *Aquac Nutr*. 2022;2022:8952755. <https://doi.org/10.1155/2022/8952755>.
70. Alharbi SA, Ovchinnikov DA, Wolvetang E. Leucine-rich repeat-containing G protein-coupled receptor 5 marks different cancer stem cell compartments in human Caco-2 and LoVo colon cancer lines. *World J Gastroenterol*. 2021;27(15):1578–94. <https://doi.org/10.3748/wjg.v27.i15.1578>.
71. Lea T. Caco-2 cell line. In: Verhoeckx K, Cotter P, López-Expósito I, Kleiveland C, Lea T, Mackie A, et al., editors. *The impact of food bioactives on health: in vitro and ex vivo models*. Cham: Springer; 2015. p. 103–11.
72. Kim S, Shin YC, Kim TY, Kim Y, Lee YS, Lee SH, et al. Mucin degrader *Akkermansia muciniphila* accelerates intestinal stem cell-mediated epithelial development. *Gut Microbes*. 2021;13(1):1–20. <https://doi.org/10.1080/19490976.2021.1892441>.
73. Macia L, Tan J, Vieira AT, Leach K, Stanley D, Luong S, et al. Metabolite-sensing receptors GPR43 and GPR109A facilitate dietary fibre-induced gut homeostasis through regulation of the inflammasome. *Nat Commun*. 2015;6:6734–49. <https://doi.org/10.1038/ncomms7734>.